

PREDICTIONS FOR A LOW-MASS CUTOFF FOR THE PRIMORDIAL BLACK HOLE MASS SPECTRUM

JAMES BARBIERI[†]

Advanced Systems Development
1 Administrative Circle, China Lake, 93555, USA

GEORGE CHAPLINE

Space Science Institute, Lawrence Livermore National Laboratory
7000 East Ave., Livermore, CA 94500, USA

*Received 16 July 2024, accepted 5 November 2024,
published online 22 November 2024*

In this note, we outline how a modest violation in the conservation of mass during the merger of two PBHs affects the PBH mass spectrum that we previously obtained using a Boltzmann equation model for the evolution of the mass spectrum with no mass loss. We find that if the initial cosmological redshift is of the order of 10^{12} , then the fraction of primordial holes with masses greater than 10^3 solar masses appears to be close to what is required to provide the seeds for galaxies. In addition, we note that as a result of rapid collisions and strong coupling to electromagnetic radiation for temperatures $> \text{GeV}$, there will be an effective low-mass cutoff in the mass spectrum for PBH masses less than a certain PBH mass less than $0.1M_{\odot}$. We also point out that this cutoff in the mass spectrum below $\sim 0.1M_{\odot}$ can be confirmed by combining future microlensing observations from the Roman Space Telescope and the Vera C. Rubin Observatory with astrometric observations.

DOI:10.5506/APhysPolB.55.10-A3

1. Introduction

Primordial black holes (PBHs) provide an attractive explanation for dark matter in that they cannot only provide the seeds for both galaxies and the large-scale density inhomogeneities in the observed universe, but because

[†] Retired.

BHs can possess a large entropy, then PBHs may explain the origin of the CMB see, *e.g.*, for a review [1]. In particular, if the cosmological redshift extends to $z \sim 10^{12}$ and the initial mass spectrum for PBHs is restricted to masses between $0.01M_{\odot}$ and $< 1M_{\odot}$, then it turns out that the appearance of a CMB and large-scale inhomogeneous structure of the universe would necessarily follow [2]. The signature for this scenario is that today there is a sharp cutoff in the PBH mass spectrum somewhere in the range $0.01\text{--}0.1M_{\odot}$.

In a previous paper [3], we introduced a Boltzmann equation formalism for evaluating how the mass spectrum of PBHs evolves with cosmological time as a result of collisions and coalescence between black holes during the long period $z < 10^{10}$ when the standard cosmological model containing radiation and dark matter is applicable. A notable consequence of our Boltzmann equation model and the assumption that dark matter consists entirely of PBHs is that the fraction of the dark matter PBH which appears with masses $> 1000M_{\odot}$ is completely consistent with the assumption that these large-mass PBHs became the seeds for galaxies and stellar clusters. In this paper, we consider how our previous model for the PBH mass spectrum is modified if during mergers the sum of the masses of the merging BHs is reduced due to gravitational radiation or radiation of entropy [4, 5].

Collisions between black holes in which the black holes do not coalesce will also result in a change in their masses due to gravitational radiation and entropy loss. However, these mass losses will be much greater when the black holes actually coalesce. In this paper, we neglect this effect, which significantly simplifies the Boltzmann equation calculation. In particular, we only include the first term in Eq. (1) which describes how the fraction of PBHs with a mass between M and $M + dM$ increases with time and due to the coalescence of a black hole of mass M' and $M - M' + \Delta M_{\text{GR}}$, where ΔM_{GR} is the mass loss due to gravitational radiation plus entropy loss.

The existence of mass loss during mergers of BHs as a result of gravitational radiation or entropy loss is, among the black hole transformations, allowed by Christodoulou [6]. In addition, the existence of mass loss during mergers of BHs appears to be consistent with LIGO observations [7]. In addition, a strong coupling between BHs and thermal radiation is expected for temperatures $> \text{GeV}$ in a quantum theory of gravity [5]. In this paper, the effect of mass loss due to either gravitational radiation or the creation and loss of BH entropy created during collisions is accounted for by simply introducing an *ad-hoc* mass loss during a merger. Since neither the amount of gravitational radiation nor entropy generation associated with the merger of two black holes can be calculated due to a lack of detailed understanding of how these mass losses depend on the initial conditions, we simply reran our Boltzmann equation model with the additional *ad-hoc* assumption that the final mass differs from the merging black holes by a deficit ΔM_{GR} . We

have considered values for ΔM_{GR} in the range of 15%–30% since these mass changes seem to be reasonable based on the LIGO data. In the future, observations of the “ring-down” gravitational signatures in the LIGO data may provide a much better understanding of the mass loss magnitudes expected for mergers of BHs with masses $> M_{\odot}$.

2. Boltzmann equation model for mass spectrum

The Boltzmann equation suggested in [3] is

$$\frac{dp(M)}{dt} = 27\pi\nu(t)\frac{\rho_{\text{DM}}}{M(t)} \left[\int_{M^*}^M \sigma_{\text{cap}}(M', M - M') p(M - M') p(M') dM' - p(M) \int_{M^*}^{\infty} \sigma_{\text{cap}}(M, M') p(M') dM' \right], \quad (1)$$

where ρ_{DM} is the present-day dark matter density, $\nu(t)$ is the virial velocity of the at time t , M_{DM} is the initial dark energy star mass (at $z \approx 10^{12}$), and σ_{cap} is the Bae cross section. Here time runs from a very early time corresponding to a redshift $1 + z_{\text{r}} \approx 10^{11}$ to $z = 0.0$. However, in practice, we were not able to extend our numerical solution to Eq. (1) to $z < 10^8$. The time dependence of the average relative velocity $\nu(t)$ is of course complicated. However, as a rough approximation, we will assume that $\nu^2(t)$ scales roughly as the inverse square root of the distance between PBHs.

In the Newtonian limit, the angular momentum $L = b\mu v_{\infty}$ where b is the impact parameter, μ is the reduced mass, v_{∞} is the virial velocity ν/c , and the energy E is $E = (1/2)\mu v_{\infty}^2$. The critical impact parameter b_{crit} is

$$b_{\text{crit}} = \frac{L}{\mu v_{\infty}} = \frac{L}{\sqrt{2\mu E}}. \quad (2)$$

For unequal masses, b_{crit} is [8]

$$b_{\text{crit}} = \left(\frac{340\pi}{3} \frac{m_1 m_2 (m_1 + m_2)^5}{v_{\infty}^2} \right)^{1/7}, \quad (3)$$

and the capture cross section is $\sigma_{\text{cap}} = \pi b_{\text{crit}}^2$.

Since the first term of the Boltzmann equation represents the increase in mass due to mergers, it is the only term where mass loss due to gravitational radiation or entropy generation is significant. We define the mass loss term $M_t(j)$ as

$$M_t(j) = \sigma_{\text{cap}}(t)\rho(t), \quad (4)$$

where $\sigma_{\text{cap}}(t)$ is the Bae cross section at time t and $\rho(t)$ is the density at time t . The change in the mass $\Delta M_t(j)$ is

$$\Delta M_t(j) = \frac{pc_{\text{loss}}}{\delta t} M_t(j), \quad (5)$$

where $M_t(j)$ is the mass array $M(j)$ at time t , and the change in mass at each time step $\delta t = t_i - t_{i-1}$, (in our implementation, $\delta t = 0.0532$ at $z = 1.0 \times 10^{12}$ to $\delta t = 33.54$ at $z = 1.0 \times 10^9$), and pc_{loss} is the estimated percent loss in mass. The updated mass due to mass loss is

$$M_t(j) = M_{t-1}(j) - \Delta M_{t-1}(j), \quad (6)$$

and our mass distributions were calculated using the above mass loss scenario. In the following, we show the initial and final normalized probability density $P(M)$ for PBH mass distributions for the scenarios considered. In the following calculation, we assume that the initial mass was $M^* = 0.05M_{\odot}$ or $M^* = 0.1M_{\odot}$, both with an initial redshift $z_i = 1.0 \times 10^{12}$. Our final redshift $z_f = 1.0 \times 10^8$ is limited by the increasing computational expense of extending the numerical solution farther in time due to the small merger rate at smaller redshifts. Indeed, we have found that the spectrum changes very slowly after $z = 10^8$. Thus, it is possible to get an idea that our calculated mass spectrum is consistent with the observed abundance of seeds of galaxies as well as N -body simulations of the formation of matter homogeneities, even though our formal calculation does not extend to $z < 1000$ where structures form. As a result of these constraints, the mass range we have considered include masses $0.01M_{\odot} < M < 1000.0M_{\odot}$. In this paper, we assume a 15% to 30% for the first term only, since the change in the spectrum due to the second term is expected to be much smaller.

3. Mass loss and entropy

Hawking's area rule [9] states that the total area of a group of black holes represents an entropy that never decreases. On the other hand, the mass of two black holes can decrease due to gravitational radiation, as well as the radiation of BH entropy as thermal electromagnetic radiation. However, the specific heat of black holes is very large [5] which implies that the temperature arising from the mergers of two BHs with masses greater than $1M_{\odot}$ is very low. Therefore, it is not expected that mass loss due to radiation of thermal entropy will be important for these masses. A similar conclusion follows from Hawking's area rule even though the specific heat implied by Hawking's entropy contradicts the requirement that the specific heat of any physical system with many degrees of freedom must be positive.

What is possible, though, is that at the cosmological red shifts, we are contemplating (*viz.* $> 10^{10}$), the contribution to mass loss of thermal radiation due to quantum effects can be important [5]. As a result, we expect that large mass losses due to both gravitational radiation and thermal heat radiation will be very important for cosmological redshifts $\gtrsim 10^{12}$, leading to a sharp cutoff in the mass spectrum for PBH masses somewhere below $1M_{\odot}$. For PBH mergers with a mass greater than M_{\odot} , we do not expect that BH entropy loss will lead to an observable mass loss, although gravitational radiation will continue to be observable.

The fact that mass increases are not observed in the LIGO events shows that the contribution of entropy generation to the mass of a black hole formed by the merger of two black holes [6] is not significant — at least for stellar masses. Of course, this is consistent with the fact that the kinetic energy of PBHs, say at $z < 1000$, will be very small compared with their mass energy. In the case of redshifts very close to the Big Bang — say $z > 10^{10}$, the internal energy created by mergers may be comparable or even larger than their rest energy. In our calculation, we will take this possibility into account by choosing an initial mass for the PBHs that is fixed by the ratio of the CMB energy density to the DM density extrapolated from the current time to the chosen initial cosmological redshift. After this initial redshift, we neglect the effect of entropy generation and mass loss during mergers.

4. Results

For the results plotted here we use as an estimate of the coefficient of Eq. (1)

$$10^{12}(1+z)^3\nu(t)\frac{\rho_{\text{DM}}}{\bar{M}(t)}\left(\frac{G}{c^2}\right)^2. \quad (7)$$

In Fig. 1, $P(M)$ distributions for $m^* = 0.1$ and $m^* = 0.05$ — assuming no mass loss — are shown. In Figs. 2 and 3, the results of the Boltzmann mass loss calculation for $m^* = 0.05M_{\odot}$ and $m^* = 0.1M_{\odot}$, for no loss, 15% mass loss, and 30% mass loss are presented.

In Figs. 2 and 3, we show the mass spectrum $P(M)$ and the mass loss spectrum as a function of the initial mass. The $P(M)$ spectrums are compared, assuming a starting masses of $m^* = 0.05M_{\odot}$ and $m^* = 0.1M_{\odot}$, and where the initial probability is calculated assuming $P(M) = (m^*/M')/\log(M_{\text{max}}/m^*)$ and $M_{\text{max}} = 10M_{\odot}$. Figures 2 and 3 suggest that the largest change between the initial and final PBH mass spectrum is in the 10^{-2} – 10^0M_{\odot} . Indeed, our mass-loss mechanism leads to a predicted low-mass cutoff of the PBH mass spectrum at $\lesssim 10^{-2}M_{\odot}$. Therefore, any observational constraints on sub-stellar mass dark compact objects may provide information relating to the origin of dark matter under our mass-loss models.

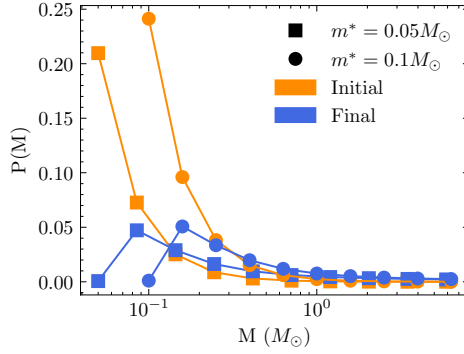


Fig. 1. $P(M)$ distributions assuming no mass loss.

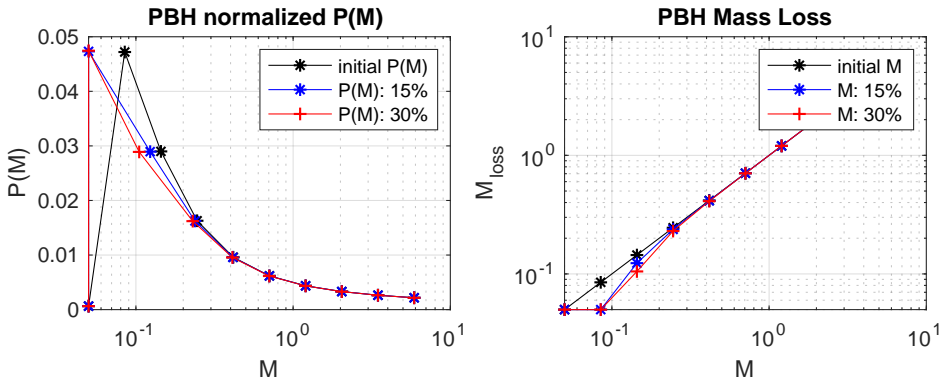


Fig. 2. $P(M)$ for $m^* = 0.05M_\odot$ for 15% and 30% mass losses.

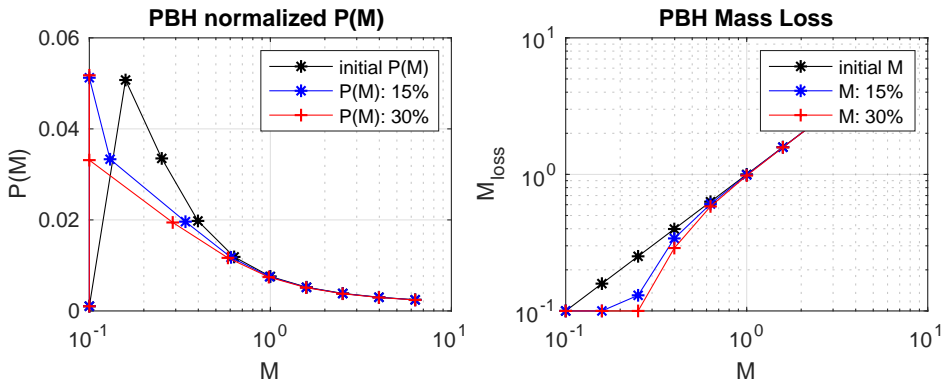


Fig. 3. $P(M)$ for $m^* = 0.1M_\odot$ for 15% and 30% mass losses.

As we noted above, the initial redshifts for our calculation were chosen to allow for the abundance of PBHs with masses $> 1000M_\odot$ to match the observed abundance of seeds for galaxies. The PBH masses were then chosen to be consistent with the horizon mass

$$M_H = 4\pi\rho R_H^3, \quad (8)$$

where R_H is the distance to the horizon ($= 3t$ in a radiation-dominated universe). This mass is relevant because in the early universe, BHs tend to form at the horizon [4]. The initial PBH mass can then be estimated using the extrapolated density of dark matter and the frequency for quanta where the event horizon becomes opaque to thermal radiation [5]

$$\nu = 0.3 \text{ GeV} \left(\frac{M_\odot}{M_{\text{BH}}} \right)^{1/2}. \quad (9)$$

In other words, when the extrapolated CMB temperature reaches $\approx 1 \text{ GeV}$, then a PBH can radiate all of its mass attributable to its internal entropy [5]. It is interesting that the OGLE microlensing data does include several events with apparent masses below 1 solar mass [10], although it may turn out that these events represent brown dwarfs rather than PHs. It is interesting that analysis of the OGLE microlensing data does include several events with masses apparently below $1M_\odot$ [10]. At present, it is unclear whether these events represent PBHs or “brown dwarfs”.

5. Observational prospects

Photometric microlensing surveys [11] currently provide the tightest constraints on compact dark object dark matter in the sub-stellar mass ranges. Observations of short-timescale photometric microlensing events towards the Galactic Bulge [12] and M31 [13] place constraints on the fraction of dark matter in PBHs at $\lesssim 10\%$ and $\lesssim 1\%$ for the mass ranges $[10^{-6}-10^{-3}]M_\odot$ and $[10^{-11}-10^{-6}]M_\odot$, respectively. However, the constraints towards the Bulge are sensitive to whether short timescale events are assumed to be caused by PBHs or a population of free-floating planets with similar masses [12]. Constraints from the microlensing surveys towards the Magellanic Clouds [14, 15] constrain the remaining substellar mass range $[10^{-3}-10^0]M_\odot$ ruling out the fraction of dark matter in PBHs at $\lesssim 5\%$. Although the current microlensing constraints rule out a large fraction of dark matter being in the form of PBHs [16], they are not sufficient to definitively probe a sub-stellar PBH mass spectrum cutoff.

Prospects for probing the sub-stellar PBH mass spectrum will improve with upcoming microlensing surveys. In addition to increased photometric sensitivity, for example, the Vera C. Rubin Observatory [17] could provide constraints on the fraction of dark matter in compact objects down to $\lesssim 0.1\%$ for masses in the range $[10^{-3}-10^0]M_{\odot}$ with photometric microlensing [18], however, this is strongly dependent on Galactic Bulge observing cadences chosen [19]. Future surveys will also be able to constraint more powerful microlensing observables. Simultaneous photometric monitoring of events from spatially separated observatories such as the Roman Space Telescope [20] at the second Lagrange point and ground-based surveys [21] will allow microlensing parallax to be measured for the free-floating planet mass ranges [22, 23] which could provide the means to disentangle PBHs from a free-floating planet population [10, 24, 25].

Finally, the advent of sub-mas astrometric capable observatories (*e.g.*, RST and Gaia) enables the astrometric signatures of microlensing events [26–28] to be detected which can provide direct lens-mass measurements [29–31] leading to direct constraints across the dark matter mass spectrum [32–35].

We would like to thank Peter McGill for pointing out that due to the emergence of new observing platforms, it will be possible to confirm the existence of a lower bound on PBH masses in the near future. We would like to thank Scott Perkins for comments regarding the interpretation of the OGLE microlensing data as well as the compatibility of our results with the LIGO observations. One of us (G.C.) would like to thank the Lawrence Livermore National Laboratory for financial support under Contract DE.AC52-07NA27344.

REFERENCES

- [1] A.M. Green, B.J. Kavanagh, «Primordial black holes as a dark matter candidate», *J. Phys. G: Nucl. Part. Phys.* **48**, 043001 (2021).
- [2] G.F. Chapline, J.F. Barbieri, «Was There a Negative Vacuum Energy in Your Past?», *J. Modern Phys.* **10**, 1166 (2019).
- [3] G.F. Chapline, J.F. Barbieri, «MACHO Messages from the Big Bang», *Lett. High Energy Phys.* **1**, 17 (2018), [arXiv:1801.07345 \[gr-qc\]](https://arxiv.org/abs/1801.07345)
- [4] G.F. Chapline, «Hadron physics and primordial black holes», *Phys. Rev. D* **12**, 2949 (1975).
- [5] G.F. Chapline, E. Hohlfield, R.B. Laughlin, D. Santiago, «Quantum phase transitions and the breakdown of classical general relativity», *Philos. Mag. B* **81**, 235 (2001).

- [6] D. Christodoulou, «Reversible and Irreversible Transformations in Black-Hole Physics», *Phys. Rev. Lett.* **25**, 1596 (1970).
- [7] M. Isi *et al.*, «Testing the No-Hair Theorem with GW150914», *Phys. Rev. Lett.* **123**, 111102 (2019).
- [8] E.D. Kovetz, «Probing Primordial Black Hole Dark Matter with Gravitational Waves», *Phys. Rev. Lett.* **119**, 131301 (2017).
- [9] L. Susskind, J. Lindsay, «An Introduction to Black Holes, Information and the String Theory Revolution: The Holographic Universe», *World Scientific*, Singapore 2005.
- [10] S.E. Perkins *et al.*, «Disentangling the Black Hole Mass Spectrum with Photometric Microlensing Surveys», *Astrophys. J.* **961**, 179 (2024).
- [11] A. Udalski, M.K. Szymanski, G. Szymanski, «OGLE-IV: Fourth Phase of the Optical Gravitational Lensing Experiment», *Acta Astronom.* **65**, 1 (2015), [arXiv:1504.05966 \[astro-ph.SR\]](#).
- [12] H. Niikura *et al.*, «Constraints on Earth-mass primordial black holes from OGLE 5-year microlensing events», *Phys. Rev. D* **99**, 083503 (2019).
- [13] H. Niikura *et al.*, «Microlensing constraints on primordial black holes with Subaru/HSC Andromeda observations», *Nat. Astron.* **3**, 524 (2019).
- [14] P. Tisserand *et al.*, «Limits on the Macho content of the Galactic Halo from the EROS-2 Survey of the Magellanic Clouds», *Astron. Astrophys.* **469**, 387 (2007).
- [15] L. Wyrzykowski *et al.*, «The OGLE view of microlensing towards the Magellanic Clouds — IV. OGLE-III SMC data and final conclusions on MACHOs», *Mon. Not. R. Astron. Soc.* **416**, 2949 (2011).
- [16] S. Bird *et al.*, «Snowmass2021 Cosmic Frontier White Paper: Primordial black hole dark matter», *Phys. Dark Universe* **41**, 101231 (2023).
- [17] Z. Ivezić *et al.*, «LSST: From Science Drivers to Reference Design and Anticipated Data Products», *Astrophys. J.* **873**, 111 (2019).
- [18] A. Drlica-Wagner *et al.*, «Probing the Fundamental Nature of Dark Matter with the Large Synoptic Survey Telescope», [arXiv:1902.01055 \[astro-ph.CO\]](#).
- [19] N.S. Abrams *et al.*, «Microlensing Discovery and Characterization Efficiency in the Vera C. Rubin Legacy Survey of Space and Time», [arXiv:2309.15310 \[astro-ph.IM\]](#).
- [20] D. Spergel *et al.*, «Wide-Field Infrared Survey Telescope-Astrophysics Focused Telescope Assets WFIRST-AFTA 2015 Report», [arXiv:1503.03757 \[astro-ph.IM\]](#).
- [21] I. Kondo *et al.*, «Prediction of Planet Yields by the PRime-focus Infrared Microlensing Experiment Microlensing Survey», *Astron. J.* **165**, 254 (2023).
- [22] S. Refsdal, «On the Possibility of Determining the Distances and Masses of Stars from the Gravitational Lens Effect», *Mon. Not. R. Astron. Soc.* **134**, 315 (1966).

- [23] A. Gould *et al.*, «Masses for free-floating planets and dwarf planets», *Res. Astron. Astrophys.* **21**, 133 (2021).
- [24] K. Pruet *et al.*, «Primordial Black Hole Dark Matter Simulations Using PopSyCLE», *Astrophys. J.* **970**, 169 (2024), [arXiv:2211.06771 \[astro-ph.GA\]](#).
- [25] C.Y. Lam *et al.*, «PopSyCLE: A New Population Synthesis Code for Compact Object Microlensing Events», *Astrophys. J.* **889**, 31 (2020).
- [26] M.A. Walker, «Microlensed Image Motions», *Astrophys. J.* **453**, 37 (1995).
- [27] E. Hog, I.D. Novikov, A.G. Polnarev, «MACHO photometry and astrometry», *Astron. Astrophys.* **294**, 287 (1995).
- [28] M. Miyamoto, Y. Yoshi, «Astrometry for Determining the MACHO Mass and Trajectory», *Astron. J.* **110**, 1427 (1995).
- [29] K.C. Sahu *et al.*, «An Isolated Stellar-mass Black Hole Detected through Astrometric Microlensing», *Astrophys. J.* **933**, 83 (2022).
- [30] C.Y. Lam *et al.*, «An Isolated Mass-gap Black Hole or Neutron Star Detected with Astrometric Microlensing», *Astrophys. J. Lett.* **933**, L23 (2022).
- [31] P. McGill *et al.*, «First semi-empirical test of the white dwarf mass–radius relationship using a single white dwarf via astrometric microlensing», *Mon. Not. R. Astron. Soc.* **520**, 259 (2023).
- [32] K. Van Tilburg, A.-M. Taki, N. Weiner, «Halometry from astrometry», *J. Cosmol. Astropart. Phys.* **2018**, 041 (2018).
- [33] H. Verma, V. Rentala, «Astrometric microlensing of primordial black holes with Gaia», *J. Cosmol. Astropart. Phys.* **2023**, 045 (2023).
- [34] C. Mondino *et al.*, «Astrometric weak lensing with Gaia DR3 and future catalogs: searches for dark matter substructure», *Mon. Not. R. Astron. Soc.* **531**, 632 (2024), [arXiv:2308.12330 \[astro-ph.CO\]](#).
- [35] J. Fardeen *et al.*, «Astrometric Microlensing by Primordial Black Holes with The Roman Space Telescope», *Astrophys. J.* **965**, 138 (2024), [arXiv:2312.13249 \[astro-ph.GA\]](#).